journal

J. Am. Ceram. Soc., 87 [7] 1306–1313 (2004)

Fracture Toughness Measurement of Chromium Nitride Films on Brass

Saki Krishnamurthy*,† and Ivar E. Reimanis*

Metallurgical and Materials Engineering Department, Colorado School of Mines, Golden, Colorado 80401

John Berger

Engineering Division, Colorado School of Mines, Golden, Colorado 80401

Elizabeth Drexler

Materials Reliability Division, National Institute for Standards and Technology, Boulder, Colorado 80305

Two methods of measuring the fracture toughness of films are critically examined using well-characterized films of CrN and Cr_2N ~6 μm in thickness bonded to brass. The first method invokes a model developed by Beuth and Klingbeil in which the film fracture stress is related to the fracture energy through an expression that accounts for work hardening of the substrate. The second method is to directly measure the displacement field around the crack tip using electron-beam moiré and, subsequently, to estimate the crack-tip stress intensity factor using full-field-displacement equations. The films are prepared by magnetron sputtering on brass substrates heat-treated at various temperatures, thereby altering the microstructure and, hence, the substrate yield stress. Unexpectedly, the same films deposited on various substrates lead to very different in-plane compressive residual stresses. The effect on crack-driving force is discussed, and a comparison between these two methods is made. Both techniques agree reasonably well and reveal that CrN exhibits a higher toughness than Cr_2N.

I. Introduction

THERE have been many attempts to establish repeatable fracture toughness (K_C) measurement techniques for thin films with the objective that K_C can be used as an engineering design parameter in the same way it is for bulk materials.[1–8] Applications where the fracture behavior of brittle films on ductile substrates may determine component survival include wear-resistant coatings for tools and dies,[9] dental coatings,[10,11] and oxide superconductor films.[12,13] In all these applications, it would be of great use to measure reliably the fracture resistance of the brittle film. A direct measurement of the strain required to propagate a crack across a film is exceedingly difficult because of challenges in obtaining a free-standing film that contains a sharp precrack. Alternatively, methods in which the substrate is loaded in tension until the film fractures are experimentally less challenging, but they are plagued with lack of understanding how stress is transferred from the substrate to the film. This is particularly challenging when the substrate exhibits elastic–plastic behavior during tensile loading, as is true for many of the above applications.

Beuth and Klingbeil[14] have developed an expression for the energy release rate of a crack channeling through a film that is well bonded to a ductile substrate for the configuration shown in Fig. 1. This is a modification of earlier models that do not consider plasticity[15] or work hardening.[16,17] If the crack is within the steady-state zone, free from film edge effects, the energy release rate for the crack is

$$G = \frac{\pi \varepsilon_c^2 E_f h}{2} g\left(\alpha, \beta, \frac{\sigma}{\sigma_y}, n\right) \quad (1)$$

where ε_c is the strain in the film when the crack propagates, h the film thickness, E_f the Young's elastic modulus of the film, g a numerically determined parameter dependent on α and β (which are Dundurs' parameters[18]), and σ_y and n the yield stress and stress exponent, respectively; the ratio σ/σ_y must be determined for a particular constitutive response. The plastic constitutive response is described by

$$\frac{\varepsilon}{\varepsilon_y} = \frac{\sigma}{\sigma_y} + \alpha\left(\frac{\sigma}{\sigma_y}\right)^n \quad (2)$$

where ε is the strain, ε_y the strain at yield, and σ the stress in the substrate. Thus, if the substrate constitutive properties are well-known and if the elastic properties of the film and substrate are known, Eq. (1) requires only that a measurement of ε_c be made. In the present work, *in situ* optical and *in situ* SEM techniques are used to detect the first crack, which is correlated to the substrate strain. Before the film cracks, an isostrain condition between the substrate and film prevails, and, thus, only a measurement of the substrate strain at cracking is necessary to obtain ε_c.

Direct measurement of the displacement field around the crack tip just before crack advancement is an alternative method to obtain the fracture toughness. The near-field equations derived by Irwin[19] adequately describe the stress field in a small region

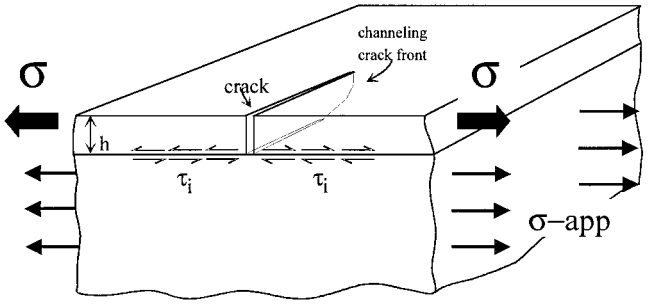

Fig. 1. Schematic showing the configuration of crack channeling through a brittle film on a ductile substrate.

M. Thouless—contributing editor

Manuscript No. 10469. Received August 15, 2003; approved February 24, 2004.
Supported by the U.S. National Science Foundation under Grant No. DMR-0103385 in the Ceramics Program.

*Member, American Ceramic Society.

†Current address: Exponent Failure Analysis Associates, 3401 Market Street, Suite 300, Philadelphia, PA 19104.

around the crack tip, but they are not sufficient if there exists a substantial fracture process zone.[20] Higher-order terms in the field equations are generally required to make use of experimental data collected outside the *K*-dominated zone. For the *u*-field displacements (those parallel to the crack plane), the full displacement field can be expressed as[21]

$$
\begin{aligned}
Eu = & \sum_j A_j r^{j+1/2}\left[\frac{1-\nu}{j+1/2}\cos(j+1/2)\theta\right. \\
& \left. -(1+\nu)\sin\theta\sin(j-1/2)\theta\right] \\
& + \sum_m B_m r^{m+1}\left[\frac{2}{m+1}\cos(m+1)\theta\right. \\
& \left. -(1+\nu)\sin\theta\sin m\theta\right] \\
& + \sum_m D_m r^{m+1}\left[\frac{1-\nu}{m+1}\sin(m+1)\theta\right. \\
& \left. +(1+\nu)\sin\theta\cos m\theta\right] \\
& + \sum_j C_j r^{j+1/2}\left[(1+\nu)\sin\theta\cos(j-1/2)\theta\right. \\
& \left. +\left(\frac{2}{j+1/2}\right)\sin(j+1/2)\theta\right] \qquad (3)
\end{aligned}
$$

where E is Young's elastic modulus, r and θ polar coordinates describing a point away from the crack tip, ν the Poisson ratio, and A_j, B_m, D_m, and C_j coefficients. In this case, $A_0 = K_I/(2\pi)^{1/2}$, where K_I is the Mode I stress intensity factor, and, at fracture, $K_I = K_C$, the fracture toughness. A similar expression exists for the *v*-direction (perpendicular to the crack plane). Equation (3) considers Mode I and Mode II loading. Barker *et al.*[21] describe a least-squares method for extracting the coefficients in Eq. (3) from moiré fringe data. Barker *et al.* also have found that the *u*-field displacement equations result in a slightly more accurate expression of *K* than do the *v*-field equations; the difference is attributable to a difference in the contribution from Poisson's contraction. The *u*-field expression, Eq. (3), is used in the present work to determine K_I.

For the latter method, one method to obtain the displacement fields is electron-beam (E-beam) moiré.[22,23] E-beam moiré was initially developed because it provided higher resolution than optical moiré interferometry (OMI) methods could offer at the time. Since then, techniques, such as phase-shifting, have substantially improved the ultimate resolution in OMI. In E-beam moiré, a crossline grating is typically placed via lithographic techniques on the sample surface, and the reference grid is the E-beam in the SEM. Thus, unlike OMI, the sample can be viewed in the normal secondary-electron mode while collecting the moiré data, which allows a direct correlation between small-scale features on the sample surface and surface displacement. Compared with OMI, E-beam moiré also does not have caustic problems near the crack tip and faces, thereby allowing a smaller zone for displacement data collection. For thin films, where the zone of data collection is on the order of the film thickness, this is an advantage. Difficulties include beam stability, magnification drift, sample alignment, and rigid-body rotation. To the knowledge of the authors, this is the first time E-beam moiré has been used to measure the crack-tip stress intensity factor. The toughness thus derived represents a film/substrate system toughness in the sense that the presence of the substrate modifies the stress field around the crack. As such, it is expected that the toughness measured using E-beam moiré is higher than that obtained from a free-standing film and correspondingly higher than that derived from the method of Beuth and Klingbeil, because the latter two methods effectively subtract the effect of the substrate. The difference between the two methods should provide a measure of the effect of the fracture process zone on toughness.

Polycrystalline chromium nitride films examined were, in part, chosen because of their use in wear-resistant coatings for metal substrates.[24] Also, it was known that CrN is more wear resistant than Cr_2N.[25,26] Thus, an objective was to establish whether or not the fracture toughness also was higher. Ideally, in assessing techniques for measuring fracture toughness, it is desirable to calibrate using a material of known fracture toughness. Unfortunately, it is difficult to create a thin film that exhibits the same microstructure and residual stress state as the same material in bulk, thereby making direct comparisons with bulk fracture toughness challenging. Therefore, the approach here is to use the consistency of both methods to examine CrN and Cr_2N films on various brass substrates as a validation of the techniques. Both techniques provide a measurement of the effective fracture toughness, namely that in the presence of a residual stress field. The "true" fracture toughness was obtained by subtracting the "effective" residual stress, as described below.

II. Experimental Procedure

Cold-rolled sheet cartridge brass of composition 70% copper and 30% zinc was used as the substrate material. The sheet was cut into tensile samples of two different gauge dimensions: 25.4 mm × 12.6 mm × 2.0 mm and 12.6 mm × 3.2 mm × 2.0 mm, as shown in Fig. 2. These samples then were annealed at various temperatures for 1 h. Stress was determined as a function of strain to evaluate the yield stress and the work-hardening exponent ($n \approx 2$).[‡] The stress–strain curves are shown in Fig. 3.

Before they were mounted in the magnetron sputtering chamber, the brass substrates were polished to a 1 μm finish using diamond paste, washed in a soap solution, and subsequently ultrasonically cleaned in acetone for 20 min. The chamber then was pumped to a vacuum $<10^{-6}$ torr (1.3×10^{-4} Pa). Two flow-rate controllers were used to monitor the amount of argon gas and nitrogen gas in the chamber during the deposition. A pure chromium target was energized using an applied voltage. Before CrN and Cr_2N were deposited, a thin (~50 nm) layer of chromium was applied to the substrate with the purpose of increasing the adhesion of the film to the substrate, as shown in earlier studies.[25] The argon gas:nitrogen gas molar ratio was kept constant at either 45:55 or 25:75, which depended on whether the desired film composition was Cr_2N or CrN, respectively.

[‡]A Ludwik constitutive description[26] describes the data slightly better than that used here (Eq. (2)), but the latter was used because Beuth and Klingbeil developed their model based on it.

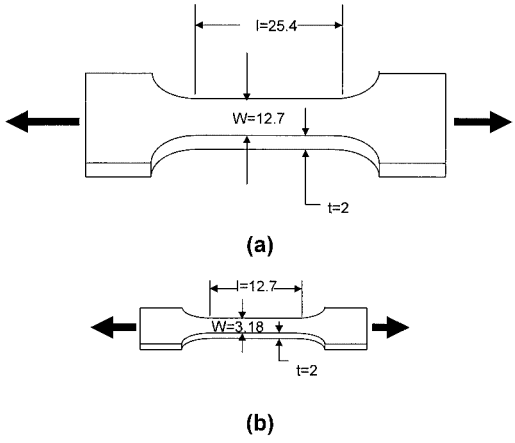

Fig. 2. Schematics showing the type of samples used for mechanical tensile tests (a) for the MTS uniaxial tester and (b) for the *in situ* SEM.

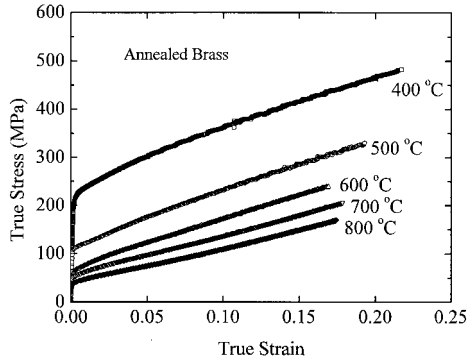

Fig. 3. True-stress–true-strain curves of brass before coating with chromium nitride, for various heat treatments.

The substrate temperature did not exceed ~150°–200°C, which was below the recrystallization temperature of brass (300°C). Most sputtering processes lasted ~35 min, the time required to obtain a 6 μm thick film. After deposition was completed, the samples were allowed to cool before they were removed from the chamber. The final film thickness (~6 μm) was measured using a diamond profilometer with a section of substrate that was masked before deposition. The stress–strain behavior of the coated substrates was almost identical to those that were uncoated; at most, the presence of the film altered stress by ~1%.[27]

XRD was used to determine film stoichiometry as well as residual stress. The glancing-angle XRD technique was used to evaluate the residual stress, using the $\sin^2 \psi$ technique. The samples were mounted on the sample holder of the diffractometer, and four glancing angles were chosen: 2°, 5°, 10°, and 15°. Silicon particles were used to calibrate the technique. The resultant stresses calculated for all the films were compressive. Two to three samples of each type were measured; results showed high repeatability.

The elastic modulus of each film was measured using a nanoindenter with a Berkovich diamond indenter tip whose displacement was depth controlled, according to Pharr and Oliver.[6] The total indentation depth did not exceed one-tenth of the film thickness.

The coated tensile samples then were gripped in a uniaxial loading frame with a 5000 lb (2.2×10^4 N) load cell or in the SEM with a 1000 lb (4.4×10^3 N) load cell. In the uniaxial loading frame, the samples were pulled in tension at a crosshead rate of 0.127 mm/min. An external 1 in. (2.54 cm) extensometer was attached to the sample to measure the macroscopic strain. To observe the formation and evolution of cracks in the film, long-range optical microscopy was used with a computer-controlled digital (CCD) camera and video recorder. In the SEM, an external controller was used to load the sample in uniaxial tension. The strain in the film was directly measured using the E-beam moiré technique, which is described in the next section. Crack initiation was recorded digitally in the form of micrographs. The change in fringe density of the micrograph with respect to a reference image gave a direct measurement of the strain at which the first cracks formed.

Preparation for viewing the film cracking using E-beam moiré was accomplished by the lithography of small grids.[28] A thin layer of gold–palladium was sputtered onto the cleaned film surface. Subsequently, a layer of polymethylmethacrylate (PMMA) was applied by spin coating. The polymer layer was heat-treated for curing at 170°C. The sample then was placed in the SEM, where the PMMA was exposed by rastering the beam at well-defined spacings to form a grid pattern. The exposure was assisted by a computer program, which maintained the location and dwell time of the electron beam. The beam current, the grid pitch, and the number of lines in the pattern were controlled by the operator. Once the grids or patterns were formed, the sample was taken out of the SEM and developed using a solution of isopropyl alcohol and methyl isobutyl ketone. The sample then was coated with a thin layer of gold–palladium so that it was electrically conductive.

Before the film was loaded, the pattern was recorded to obtain a reference image. Moiré fringe patterns in the 0° position (perpendicular to the applied load) and 90° position (parallel to the applied load) then were acquired at regular load intervals. The moiré fringes were observed at an accelerating voltage of 5 kV, working distance of 16–18 mm, and probe current of 10–20 pA, at a magnification between 800× and 1200×. The change in the density of fringes between the reference image and that obtained at a given load gave the resultant strain in the film. A fringe-tracing program was used to trace the fringes and define their centers. The crosslined grating was analogous to having a displacement gauge with full view, 0°–90°. However, the resolution of the grids was tens of nanometers, and the strains obtained from this technique were fully quantitative. In addition to direct strain measurement, this technique allowed a measurement of the displacement field around selected cracks tips. In each of four sample types, cracks that had partially channeled through the film were targeted for displacement-field measurements.

III. Results

(1) Film Characterization

In-plane compressive residual stresses were observed in the four sample types examined. Table I shows that the range of residual stress for the same film (but different substrate) is large. Also observed was a change in texture. For CrN, the texture changed from prominently (200) to (311) from the high-yield-stress substrate to the low-yield-stress substrate. Correspondingly, for Cr_2N, the (101) planes were completely dominant for the high-yield-stress substrate, and the (111)/(220) were prominent in the low-yield-stress substrate. The origin of these texture changes and their correlation to the in-plane residual stress state is not known. Also shown in Table I is the elastic modulus as evaluated using nanoindentation.

(2) Fracture Toughness Measurement

The initiation strain as a function of substrate yield stress is shown in Figs. 4(a) and (b) for CrN and Cr_2N, respectively. Measurements from optical microscopy and SEM are in agreement. Three measurements were made to obtain each data point; numerical scatter did not exceed 10%. In each case, the initiation strain exceeded the yield strain of the substrate. Each film exhibits an opposite trend, consistent with measured changes in residual stress (Table I). To better visualize the trends, the data are expressed as effective fracture toughness via Eq. (1), and using $K_C = (G_C E)^{1/2}$, assuming the film behavior is linear elastic. The modifier "effective" is used, because the compressive residual stresses in the films have not been subtracted in the calculation. For each substrate type, the value of the numerical parameter g (Eq. (1)) is uniquely determined, according to the method described in Beuth and Klingbeil[14] for work-hardening substrates. The maximum variance of g is 14% for Cr_2N but only 3% for CrN. Figures 5(a) and (b) show the fracture toughness as a function of substrate yield stress for CrN and Cr_2N, respectively. Relatively high values correspond to films that experience high residual stress (Table I).

Table I. Elastic Modulus Measured Using Nanoindentation and Residual Stress†

Film type	Substrate yield stress (MPa)	Film elastic modulus (GPa)	Residual stress (MPa)
CrN	20	380	−2300
CrN	189	380	−300
Cr_2N	20	250	−900
Cr_2N	189	250	−2400

†Measured using XRD for four different films. Thickness of CrN and Cr_2N films was 5.1 and 6.5 mm, respectively.

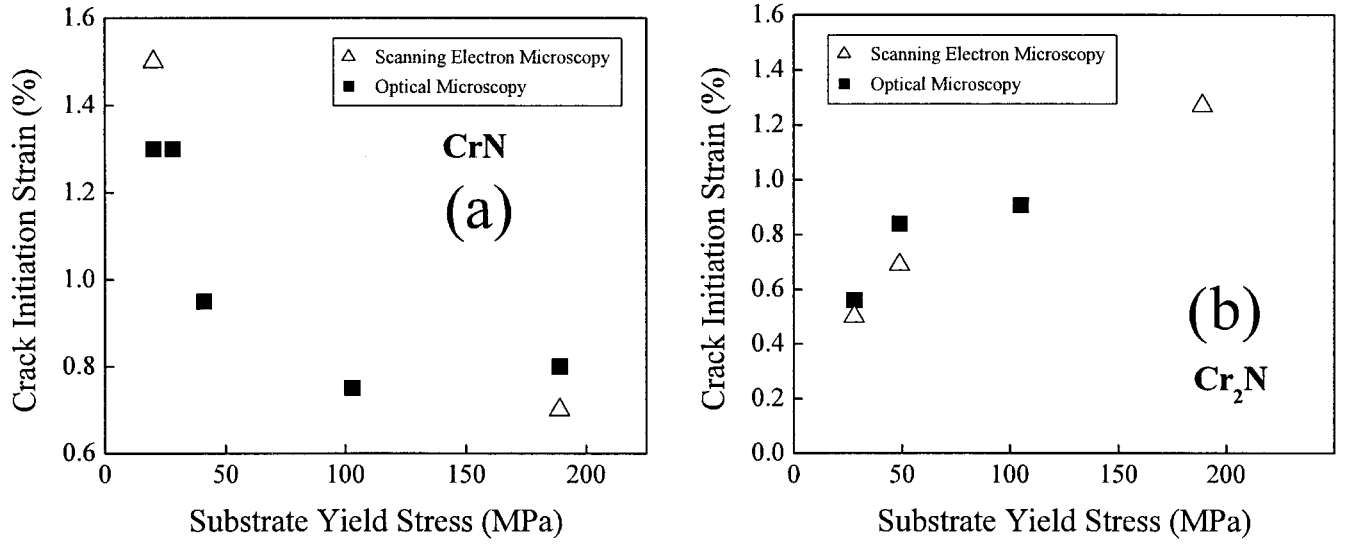

Fig. 4. Initiation strain measured as a function of yield stress for (a) CrN films and (b) Cr_2N films. *In situ* optical microscopy and SEM measurements are shown. Scattering for all data points did not exceed 10%.

For the four films where a residual stress measurement was made, the in-plane residual compressive stress could be subtracted directly from the measured crack initiation stress (assuming uniaxial loading, $\sigma_c = E\varepsilon_c$), which provided the fracture toughness for each type of film, i.e., that in the absence of residual stress. Table II presents the fracture toughness for four films, from which it is apparent that CrN is tougher than Cr_2N. It is assumed that the substrate has not yielded substantially in the presence of the large compressive residual stresses in the film (i.e., during film deposition). Thus, the value of g calculated using σ_y in Eq. (1) assumes the constitutive response given in Fig. 3. If indeed some plasticity was induced in the substrate during film deposition, then g needs to be recalculated using a new (higher) value of σ_y. However, as noted above, the largest difference in g is 14% in the case of Cr_2N for a soft ($\sigma_y = 20$ MPa, $g = 0.93$) and hard ($\sigma_y = 189$ MPa, $g = 0.80$) substrate. Based on the relative insensitivity of g to changes in yield stress, g has not been modified to include the effects of the film residual stress on the substrate plasticity.

During the E-beam moiré experiments, it was observed that cracks tended to be more stable when the film was relatively saturated with cracks. Because crack stability greatly facilitated the measurement, in all four samples for the E-beam moiré experiments, the crack was bounded on two sides by preexisting cracks that had channeled through the entire film. Although the bounding cracks may affect the applied stress field of the channeling crack, the E-beam moiré analysis is independent of the loading mode, and, thus, the presence of the cracks is not expected to introduce inaccuracies with respect to the applied load. Similarly, the presence of these cracks may introduce geometric relaxations of the residual stress, but, because the lithography is applied before the development of cracks, the relaxations should not influence the E-beam moiré measurements; they only influence the applied loads necessary to cause crack extension. Four example patterns are shown in Figs. 6, 7, 8, and 9. In each case, the pattern was obtained at a load before crack extension, and the crack propagated straight ahead. The circle in the micrograph indicates the approximate location of the crack tip. The load at which the crack extended varied but was not more than 10% higher than the load at which the data were obtained. At the critical load, the crack extended at a rate higher than could be measured for ~20 to 30 μm before arresting.

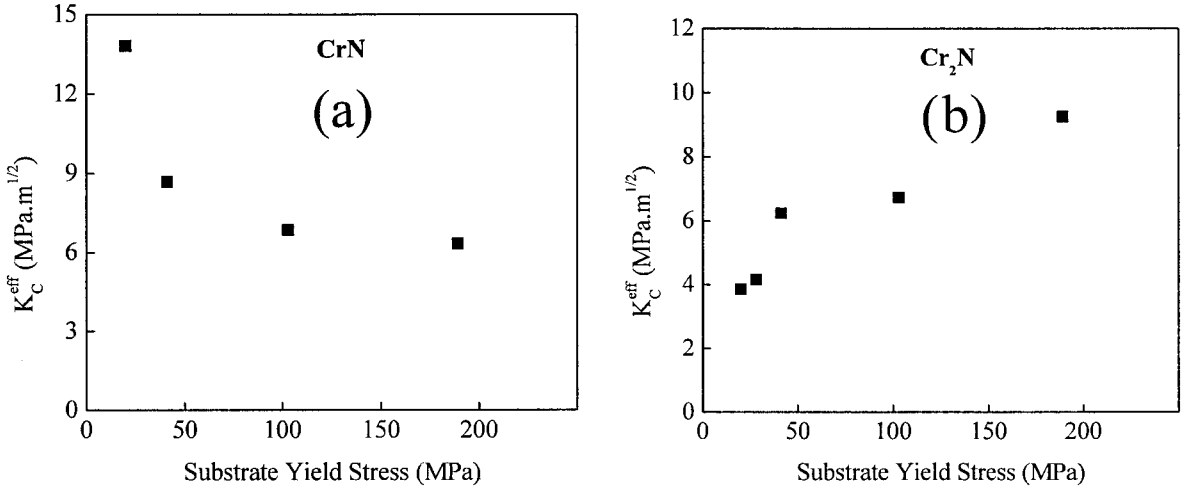

Fig. 5. Effective fracture toughness, K_C^{eff}, calculated from the method of Beuth and Klingbeil as a function of yield stress for (a) CrN and (b) Cr_2N films. Effective toughness is generally high because of the large compressive residual stresses present in the film; the large range results from the large range of residual stresses. Strain used to find each data point is shown in Fig. 4. Largest error derives from the error in measuring strain, and, thus, the errors are not expected to exceed 10%.

Table II. Effective Fracture Toughness and Fracture Toughness†

Film type	Substrate yield stress (MPa)	Effective fracture toughness ($MPa \cdot m^{1/2}$)	Fracture toughness ($MPa \cdot m^{1/2}$)
CrN	20	14	8
CrN	189	6	6
Cr_2N	20	4	1
Cr_2N	189	9	2

†Calculated from the crack-initiation strain data and applying the model of Beuth and Klingbeil for four different films. Fracture toughness was calculated by subtracting the residual stress (Table I) from the crack driving force, using Eq. (1).

The displacement field was obtained by converting the digitally acquired moiré data using the known grating frequency. The data were entered into a spreadsheet that was then used to fit Eq. (3), using the method of local collocation. The total number of terms in Eq. (3) and the total number of data points were varied independently to establish when convergence was obtained. According to Barker *et al.*,[21] best results are obtained when the number of data points is >10 times the number of terms. In this way, a mathematically stable solution results. The leading term in Eq. (3), A_0, which equals $K_I/(2\pi)^{1/2}$, is determined for each configuration. When the crack extends, $K_I = K_C^{eff}$, i.e., the effective fracture toughness. As before, the modifier "effective" is used to indicate that the films are under residual compressive stress during the crack extension experiment. Values for the effective fracture toughness obtained in this manner are given in Table III. Also shown in Table III are values of the fracture toughness (without residual stress) calculated by assuming that the residual stress is directly superposed onto the crack-tip stress field. Specifically, using Eq. (1), a hypothetical critical strain was calculated, using the E-beam moiré-derived K_I incipient to crack extension. The critical strain was converted to a critical stress, from which the residual stress (Table I) was subtracted. A new K_I then was calculated using Eq. (1). Although this back calculation for the fracture toughness is indirect, it appears to be the only method by which to remove the effect of residual stress. Table III shows that the toughness of CrN is higher than that of Cr_2N, which is consistent with the results obtained above using the method of Beuth and Klingbeil (Table II). A plot showing the results of the two methods for the four samples is shown in Fig. 10.

Unfortunately, the errors associated with the E-beam moiré technique are very difficult to quantify. Although error analyses for strain measurements using this technique have been developed,[29] error analyses for obtaining K_I from the displacement

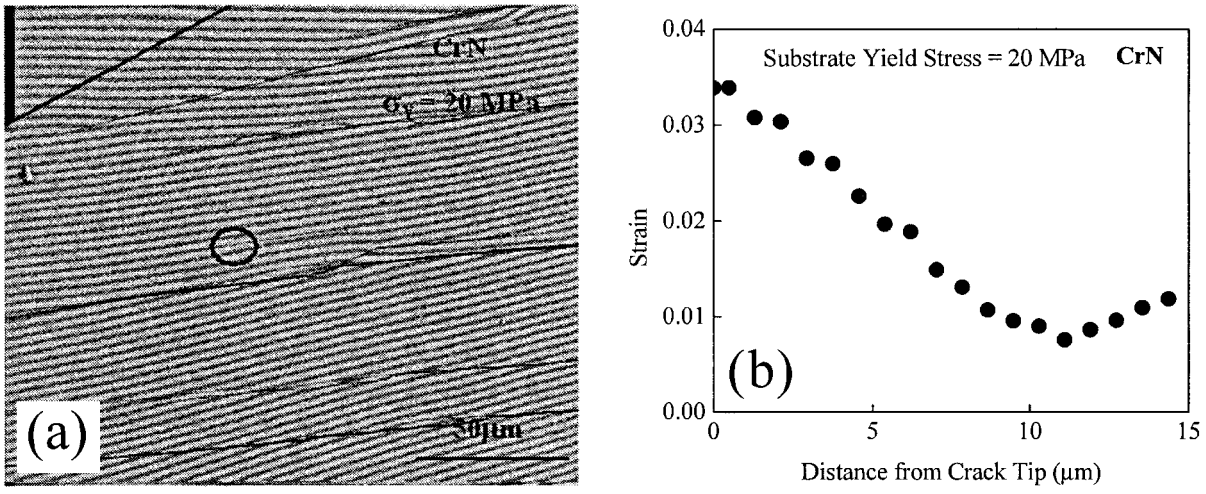

Fig. 6. (a) E-beam moiré raw pattern and (b) associated *v*-field normal strain in front of the crack tip for CrN on brass of yield stress 20 MPa. Circle in the micrograph indicates the approximate location of the crack tip. Moiré fringes are apparent as the thicker dark and evenly spaced striations. Cracks also are visible as thick dark lines.

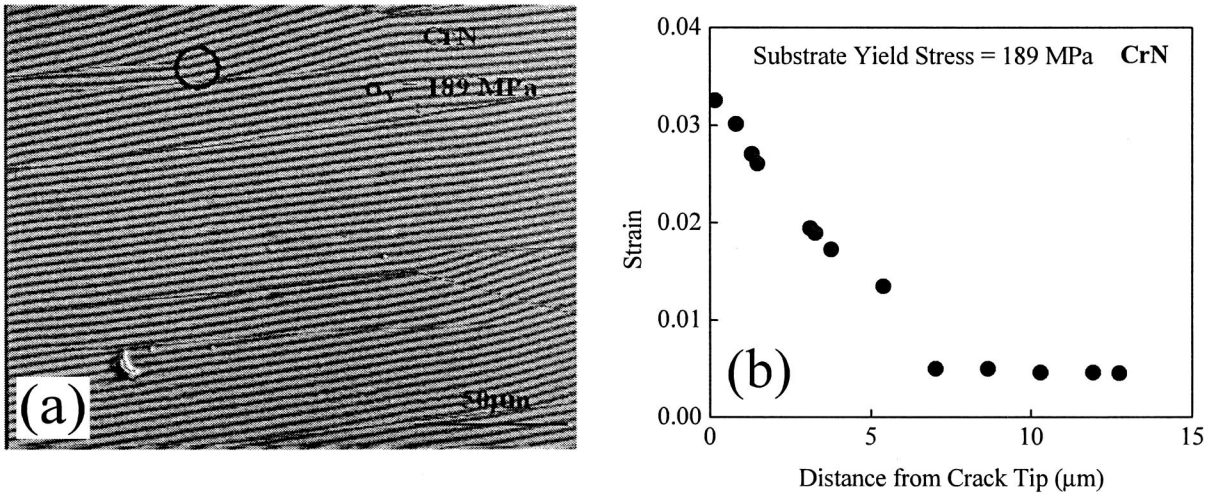

Fig. 7. (a) E-beam moiré raw pattern and (b) associated *v*-field normal strain in front of the crack tip for CrN on brass of yield stress 189 MPa. See Fig. 6 caption for a more detailed description.

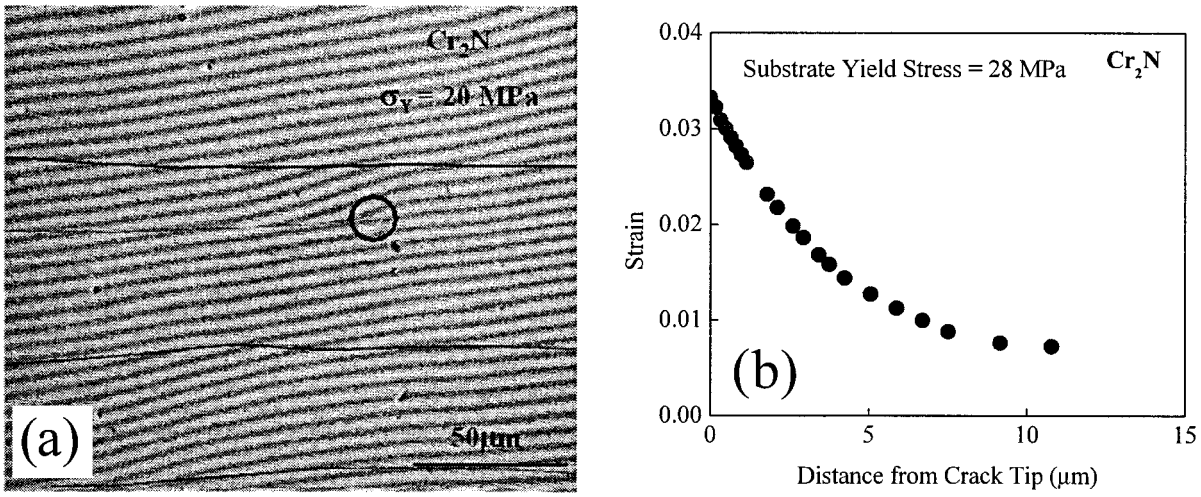

Fig. 8. (a) E-beam moiré raw pattern and (b) associated *v*-field normal strain in front of the crack tip for Cr_2N on brass of yield stress 20 MPa. See Fig. 6 caption for a more detailed description.

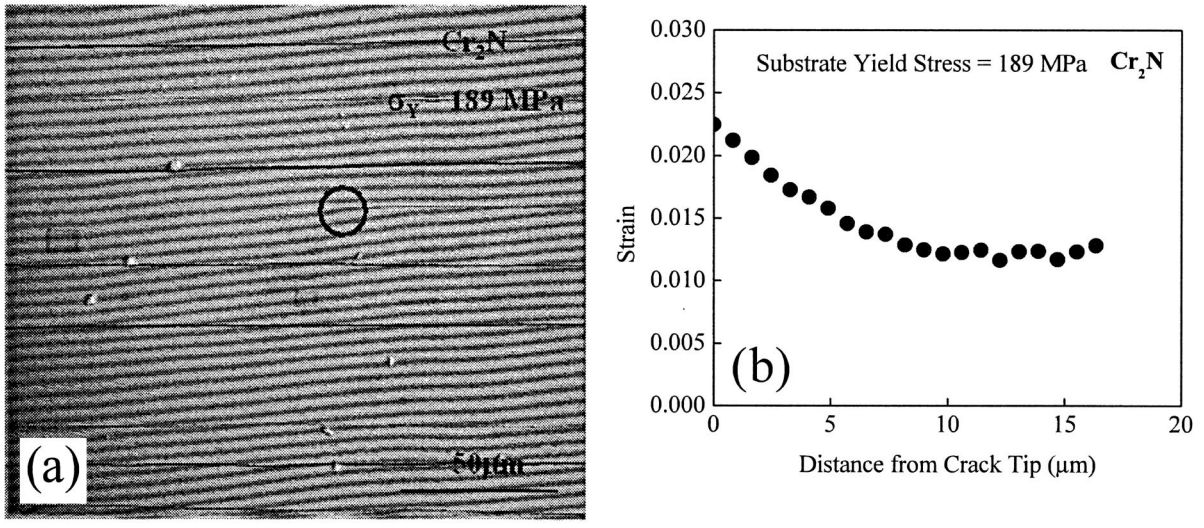

Fig. 9. (a) E-beam moiré raw pattern and (b) associated *v*-field normal strain in front of the crack tip for Cr_2N on brass of yield stress 189 MPa. See Fig. 6 caption for a more detailed description. Because of the uncharacteristic, linear strain distribution, it is concluded that the crack in this experiment may not have been well formed.

fields have not been developed. Berger *et al.*[29] have studied errors in strains determined from E-beam moiré measurements. They found that the main error source was due to magnification drift in the SEM. In uniaxial strain, the error was found to vary as the drift in magnification divided by the magnification, $\Delta M/M$. At a magnification of 1100×, the authors found an error in the strain measurement of ~3%. Here, the value of the stress intensity factor linearly scales the amplitude of the strain field. Therefore, an error of ~3% is anticipated in the K_I values because of drift of the magnification of the electron microscope.

Table III. Effective Fracture Toughness and Fracture Toughness†

Film type	Substrate yield stress (MPa)	Effective fracture toughness (MPa·m$^{1/2}$)	Fracture toughness (MPa·m$^{1/2}$)
CrN	20	21	15
CrN	189	12	12
Cr_2N	20	5	3
Cr_2N	189	8	1

†Obtained from E-beam moiré for three different films. Toughness was calculated in the same way as that in Table II, namely, the effect of residual stress was subtracted using Eq. (1), but the strain was determined by E-beam moiré using an inverse application of Eq. (1).

IV. Discussion

Both methods examined here indicate that CrN is inherently tougher than Cr_2N. Tables II and III present the fracture toughness of these two films. In all cases, the presence of compressive residual stress elevates the effective fracture toughness above the fracture toughness. Past tribological studies[25,26] indicate that CrN is more wear resistant than Cr_2N. Unfortunately, in these past tribological studies, the film residual stress state has not been determined and correlated with the wear performance, which makes a direct comparison to the present results more difficult. The hardness also is an important factor in governing wear behavior.[30] Nonetheless, based on studies that have correlated wear and toughness,[30] it is expected that a more-wear-resistant film also is tougher.

It is encouraging that both methods for evaluating the fracture toughness clearly provide the ability to distinguish between the various films. The method of Beuth and Klingbeil appears to be more accurate, because the fracture toughness falls within accepted

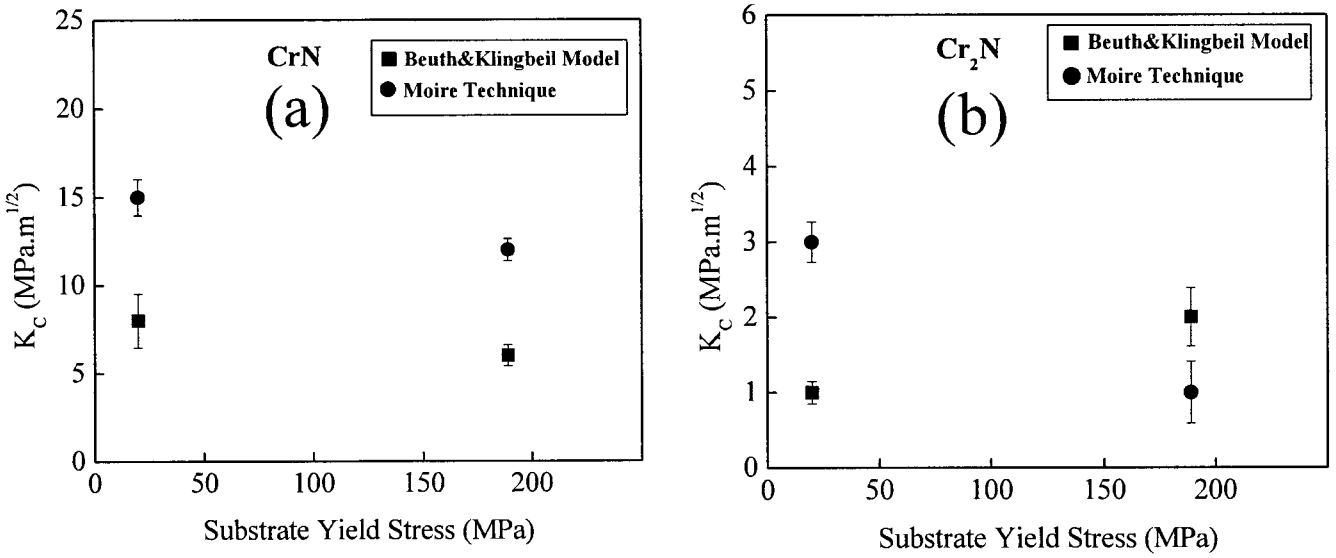

Fig. 10. Fracture toughness shown for two different substrate types comparing the method of Beuth and Klingbeil and E-beam moiré for (a) CrN and (b) Cr_2N films. Effect of residual stress has been subtracted from each of the methods.

values for ceramics (1–5 MPa·m$^{1/2}$),[30] whereas those found by E-beam moiré are high. In particular, the E-beam moiré measured value of 12–15 MPa·m$^{1/2}$ for CrN is high. There is no evidence of a crack-tip shielding mechanism, such as bridging, crack deflection, or microcracking. However, it is likely that the substrate influences the far-field crack-tip stresses in such a way as to shield the near-field crack-tip stresses. This shielding is similar to an *R*-curve effect and contributes to crack stabilization for short crack lengths. For longer cracks, such as those examined in the present study, the crack grows in a region at the plateau of the *R*-curve and is not expected to be stable. The observation that crack extension occurs in short bursts, where the crack extends ~15–30 μm when a critical load is achieved, is likely due to the perturbation of the applied stress field by the preexisting film cracks whose distribution varies across the film.

The surrounding geometry for the channeling cracks in the E-beam moiré experiments is different from that for the initiation cracks used in the Beuth and Klingbeil analysis. In particular, the former are surrounded by other cracks that have already channeled through the film (see, e.g., Figs. 6–9). These cracks may modify the channeling crack stress field. Additionally, the uncracked segment of the film may geometrically relax because of residual stresses. These geometrical relaxations may be difficult to predict if there exists a residual stress gradient through the film thickness. Finally, it has been previously shown in two-dimensional finite-element models that the uncracked segments of film may have substantial stress gradients through the film thickness during substrate loading.[31] It also has been shown in this latter study that compressive stresses can be developed on the film surface, during tensile loading. Nonetheless, these effects are not expected to influence the E-beam moiré results, because the initial null pattern, against which all the displacements are measured, is obtained before straining the substrate and, thus, before the presence of film cracks. Whether the stress to crack the film has been applied through stress transfer from the substrate to the film, or geometric stress alterations that result from film cracking, the technique yields the driving force to channel a crack through the film as it is deposited. Thus, the presence of film cracks in the E-beam moiré technique is not expected to lead to differences in measured toughness between the two techniques.

One possible source of discrepancy between the two techniques concerns the measured film elastic modulus. Results obtained by the moiré technique are sensitive to the value of Young's modulus, as shown by the left side of Eq. (3). Because the nanoindentation technique probes only a single grain, it is likely that it overestimates the effective in-plane film modulus. Specifically, a columnar film microstructure is expected to be more compliant than single grains or bulk material. Additionally, the Poisson's ratio is likely different.

A thorough characterization of the film microstructure and composition is probably necessary to explain differences between the two techniques. Such a study also is necessary to explain why the substrate strongly affects the residual stress state in the films, and why the trend is opposite for the two different films (Figs. 4 and 5). The intrinsic stresses developed during film deposition must depend on the substrate grain size and texture. The relation of the substrate microstructure to the growth processes is different for CrN and Cr_2N. Furthermore, if residual stress gradients through the thickness do exist, then their magnitude likely depends on the type of film. Accordingly, the measurement of residual stress using glancing-angle XRD (Table I) strongly depends on the total film thickness. A complete characterization of the residual stress gradient ultimately is necessary to properly assess how residual stress modifies the effective fracture toughness.

V. Conclusions

Film fracture toughness has been measured using two independent techniques on a variety of chromium nitride films on brass substrates. In both techniques, the effect of residual stress on the effective fracture toughness has been examined. One technique is based on a method best described by Beuth and Klingbeil,[14] in which the crack initiation strain is related to the energy release rate for a channeling crack. In the other technique, crack-tip displacement fields are measured using E-beam moiré, and the stress intensity factor is obtained using displacement field equations. In the latter, it is likely that the stress intensity factor for the crack in the film is elevated because of the presence of the substrate. As such, the E-beam moiré technique provides a measure of how the presence of the substrate contributes to fracture resistance. Both techniques indicate that CrN exhibits a higher toughness than Cr_2N. The substrate microstructure as modified by heat treatment influences the level of in-plane residual stress in the brittle films, which subsequently affects the effective fracture toughness.

References

[1]M. Ohring, *The Materials Science of Thin Films*. Academic Press, San Diego, CA, 1992.

[2]J. S. Wang, Yu. Sugimura, A. G. Evans, and W. K. Tredway, "The Mechanical Performance of DLC Films on Steel Substrates," *Thin Solid Films*, **325**, 163–74 (1998).

[3]B. F. Chen, J. Hwang, G. P. Yu, and J. H. Huang, "*In Situ* Observation of the Cracking Behavior of TiN Coating on 304 Stainless Steel Subjected to Tensile Strain," *Thin Solid Films*, **352**, 173–78 (1999).

[4]M. Andritschky and P. Alpuim, "Strength Measurements of Thin Brittle ZrO_2 Coatings Produced by Magnetron Sputtering on Steel Substrates," *Vacuum*, **48**, 417–22 (1997).

[5]T. Ye, Z. Suo, and A. G. Evans, "Thin Film Cracking and the Role of Substrate and Interface," *Int. J. Solids Struct.*, **29**, 2639–48 (1992).

[6]G. M. Pharr and W. C. Oliver, "Measurement of Thin Film Mechanical Properties Using Nanoindentation," *MRS Bull.*, **17**, 28–33 (1992).

[7]J. Malzbender and G. de With, "Energy Dissipation, Fracture Toughness, and the Indentation Load–Displacement Curve of Coated Materials," *Surf. Coat. Technol.*, **135**, 60–68 (2000).

[8]J. H. Selverian and D. O'Neil, "Strength and Toughness Measurement of Thin Brittle Coatings on Substrates: Part I. Theory and Measurement; Part II. Experimental Determination," *Thin Solid Films*, **235**, 120–36 (1993).

[9]D. Zhong, "Synthesis, Processing, and Modeling of a Graded Coating Architecture for Glass Molding Dies and Forming Tools"; Ph. D. Thesis. Colorado School of Mines, Golden, CO, 2001.

[10]B. R. Lawn, "Ceramic-Based Layer Structures for Biomechanical Applications," *Curr. Opin. Mater. Sci.*, in press.

[11]C. Ford, M. B. Bush, and X. Z. Hu. "A Numerical Study of Contact Damage and Stress Phenomena in Curved Porcelain/Polymer Bilayers," *Compos. Sci. Technol.*, in press.

[12]N. Cheggour, J. W. Ekin, C. C. Clickner, R. Feenstra, A. Goyal, M. Paranthaman, D. F. Lee, D. M. Kroeger, and D. K. Christen, "Transverse Compressive Stress, Fatigue, and Magnetic Substrate Effects on the Critical Current Density of Y-Ba-Cu-O Coated RABiTS Tapes"; p. 461 in *Advances in Cryogenic Engineering*, CP614, Proceedings of the International Cryogenic Materials Conference (ICMC), Vol. 48. Edited by B. Balachandran *et al.*, 2002.

[13]J. W. Ekin, S. L. Bray, N. Cheggour, C. C. Clickner, S. R. Foltyn, P. N. Arendt, A. A. Polyanskii, D. C. Larbalestier, and C. N. McCowan, "Transverse Stress and Fatigue Effects in Y-Ba-Cu-O Coated IBAD Tapes," *IEEE Trans. Appl. Supercond.*, **11** [1] 3389–97, March 2001.

[14]J. L. Beuth and N. W. Klingbeil, "Cracking of Thin Films Bonded to Elastic–Plastic Substrates," *J. Mech. Phys. Solids*, **44**, 1411–28 (1996).

[15]M. D. Thouless, "Crack Spacing in Brittle Films on Elastic Substrates," *J. Am. Ceram. Soc.*, **73**, 2144–46 (1990).

[16]M. S. Hu and A. G. Evans, "The Cracking and Decohesion of Thin Films on Ductile Substrates," *Acta Metall.*, **37**, 917–25 (1989).

[17]J. L. Beuth, "Cracking of Thin Bonded Films in Residual Tension," *Int. J. Solids Struct.*, **29**, 1657–75 (1992).

[18]J. Dundurs, "Discussion of Edge-Bonded Dissimilar Orthogonal Elastic Wedges under Normal and Shear Loading," *J. Appl. Mech.*, **36**, 650–52 (1969).

[19]G. R. Irwin, "Discussion of the Dynamic Stress Distribution Surrounding a Running Crack—A Photoelastic Analysis," *Proc. Soc. Exp. Stress Anal.*, **16**, 93–96, (1958).

[20]R. Chona, G. R. Irwin, and R. J. Sanford, "Influence of Specimen Size and Shape on the Singularity-Dominated Zone," STP 791, Vol. 1, pp. I-3–I-23. American Society for Testing and Materials, West Conshohocken, PA, 1983.

[21]D. B. Barker, R. J. Sanford, and R. Chona, "Determining *K* and Related Stress Field Parameters from Displacement Fields," *Exp. Mech.*, [Dec.] 399–407 (1985).

[22]D. T. Read and J. W. Dally, "Theory of Electron Beam Moire," *J. Res. NIST*, **101**, 47–61 (1996).

[23]D. T. Read and J. W. Dally, "Electron-Beam Moire Study of Fracture of a Glass-Fiber-Reinforced Plastic Composite," *Trans. Am. Soc. Mech. Eng.*, **61**, 402–409 (1994).

[24]P. M. Fabis, R. A. Cooke, and S. McDonough, "Stress State of Chromium Nitride Films Deposited by Reactive Direct-Current Planar Magnetron Sputtering," *J. Vac. Sci. Technol.*, **A8**, 3809–18 (1990).

[25]A. M. Peters, "Development of a Model-Graded Architecture for Chromium Nitride Coatings Deposited by Cathodic Arc Evaporation for Wear Resistant and Forming Applications"; Ph.D. Thesis. Colorado School of Mines, Golden, CO, 1999.

[26]T. Dennin, "An Investigation of Cathodic Arc Evaporation of Cr–N on Aluminum"; Ph.D. Thesis. Colorado School of Mines, Golden, CO, 2003.

[27]S. Krishnamurthy, "Cracking in Chromium Nitride Coatings on Brass"; Ph.D. Thesis. Colorado School of Mines, Golden, CO, 2003.

[28]E. S. Drexler, "Procedures for Electron Beam Moire Technique"; pp. 1–14 in NIST Tech. Note 1500–2, Materials Reliability Series, NIST, Gaithersburg, MD, 1998.

[29]J. R. Berger, E. S. Drexler, and D. T. Read, "Error Analysis and Thermal Expansion Measurement with Electron Beam Moire," NIST internal report, NIST, Gaithersburg, MD, 1997.

[30]B. Lawn, *Fracture of Brittle Solids*; p. 55. Cambridge Solid-State Series, Cambridge University Press, Cambridge, U.K., 1992.

[31]S. Krishnamurthy and I. E. Reimanis, "Multiple Cracking in CrN and Cr_2N Films on Brass," *Surf. Coat. Technol.*, in press. □